Analytica Chimica Acta 1205 (2022) 339738

Contents lists available at ScienceDirect

Analytica Chimica Acta

journal homepage: www.elsevier.com/locate/aca

A novel approach for adapting the standard addition method to single particle-ICP-MS for the accurate determination of NP size and number concentration in complex matrices

Maite Aramendía [a, b, *], Juan Carlos García-Mesa [b, c], Elisa Vereda Alonso [c], Raúl Garde [b], Antonio Bazo [b], Javier Resano [d], Martín Resano [b, **]

[a] Centro Universitario de la Defensa de Zaragoza, Carretera de Huesca s/n, 50090, Zaragoza, Spain
[b] Department of Analytical Chemistry, Aragón Institute of Engineering Research (I3A), University of Zaragoza, Pedro Cerbuna 12, 50009, Zaragoza, Spain
[c] Department of Analytical Chemistry, Faculty of Sciences, University of Málaga, 29071, Málaga, Spain
[d] Department of Computer Sciences and Systems Engineering (DIIS), Aragón Institute of Engineering Research (I3A), University of Zaragoza, C/ Mariano Esquillor SN, 50018, Zaragoza, Spain

HIGHLIGHTS

- Adaptation of the standard addition calibration method for SP-ICP-MS.
- Flexible working methodology through online addition of standards via a T-piece.
- Mathematical deconvolution permits differentiating the sample and standard signals.
- Accurate sizing and counting of AuNPs dispersed in TMAH and ethanol is presented.

GRAPHICAL ABSTRACT

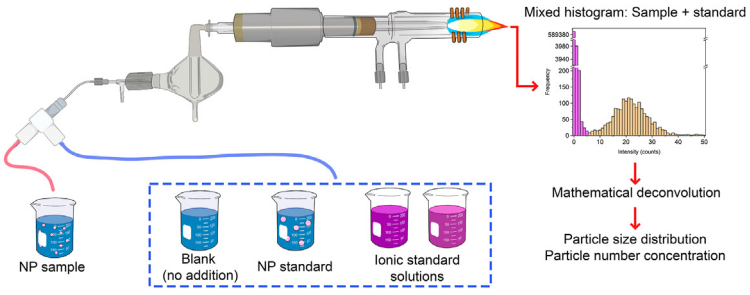

ARTICLE INFO

Article history:
Received 15 November 2021
Received in revised form
10 March 2022
Accepted 16 March 2022

Keywords:
Single particle-ICP-MS
Calibration
Matrix effects

ABSTRACT

This paper presents a novel approach, based on the standard addition method, for overcoming the matrix effects that often hamper the accurate characterization of nanoparticles (NPs) in complex samples *via* single particle inductively coupled plasma mass spectrometry (SP-ICP-MS). In this approach, calibration of the particle size is performed by two different methods: (i) by spiking a suspension of NPs standards of known size containing the analyte, or (ii) by spiking the sample with ionic standards; either way, the measured sensitivity is used in combination with the transport efficiency (TE) for sizing the NPs. Moreover, such transport efficiency can be readily obtained from the data obtained *via* both calibration methods mentioned above, so that the particle number concentration can also be determined.

The addition of both ionic and NP standards can be performed on-line, by using a T-piece with two inlet lines of different dimensions. The smaller of the two is used for the standards, thus ensuring a constant and minimal sample dilution. As a result of the spiking of the samples, mixed histograms including the signal of the sample and that of the standards are obtained. However, the use of signal deconvolution approaches permits to extract the information, even in cases of signal populations overlapping.

* Corresponding author. Centro Universitario de la Defensa de Zaragoza, Carretera de Huesca s/n, 50090, Zaragoza, Spain.
** Corresponding author.
E-mail addresses: maiteam@unizar.es (M. Aramendía), mresano@unizar.es (M. Resano).

https://doi.org/10.1016/j.aca.2022.339738

For proofing the concept, characterization of a 50 nm AuNPs suspension prepared in three different media (i.e., deionized water, 5% ethanol, and 2.5% tetramethyl ammonium hydroxide-TMAH) was carried out. Accurate results were obtained in all cases, in spite of the matrix effects detected in some media. Overall, the approach proposed offers flexibility, so it can be adapted to different situations, but it might be specially indicated for samples for which the matrix is not fully known and/or dilution is not possible/recommended.

1. Introduction

Single particle inductively coupled plasma mass spectrometry (SP-ICP-MS) emerged in the past decade as a powerful tool for nanoparticle characterization in suspensions, and has been gaining popularity in the last years due to different reasons [1,2]. SP-ICP-MS is highly sensitive, does not require extensive sample preparation and offers the capability of characterizing NPs in a fast way. This technique provides information on NP elemental composition, particle size and NP size distribution (as long as some knowledge on the NP shape and density is available or assumed), as well as particle mass and number concentration at low, environmentally relevant levels (10^6–10^8 part·L^{-1}) [3]. Additionally, it can provide information on the concentration of ionic species coexisting with the NPs in the same suspension [4]. In few years, this working methodology has passed from a development to application stage, and many papers have been published dealing with NP determination in food, cosmetics, biological tissues, animal models, soils, or waters, among others [5]. However, there are still some aspects that need further attention, especially concerning the accuracy of the particle size and particle number concentrations (PNC) determined in real, complex matrices [6,7].

Indeed, when applied to these complex samples, SP-ICP-MS can suffer from matrix effects, which degrade the quality of measurements [8]. As for conventional ICP-MS analysis, these effects can be categorized into spectral overlaps or non-spectral interferences.

The occurrence of matrix-induced spectral interferences in SP-ICP-MS results in elevated background signals with a direct impact on the NP size limits of detection (LODs). In such cases, the use of quadrupole-based ICP-MS instruments with collision/reaction cells and high-resolution sector field ICP-MS devices has proven useful [9–11].

On the other hand, matrix can also induce intensity changes in the ICP-MS response, which can compromise calibration. The most common calibration strategy currently used for determining both NP size and PNC by SP-ICP-MS consists of deploying an appropriate method to determine sample transport efficiency to the ICP (TE; the relation between the detected and aspirated mass of the target element) [12], and generating a mass-flux calibration curve with a set of standard solutions of the analyte in ionic (most frequently) or nanoparticulate [13] form. In such cases, the matrix present in the sample suspensions can affect ICP-MS detection sensitivity and/or sample transport efficiency, causing bias for the sizing and counting of the NPs [6,14]. It is fair to say at this point that using sample introduction systems with 100% TE [15,16] is also possible and potentially less affected by matrix effects [8]. In particular, the use of a microdroplet generator enables different calibration approaches since such microdroplets can be used as NP proxies [8,17], but still the application of these strategies is limited by the availability of these alternative introduction devices [18]. Although these matrix effects can be alleviated by sufficient sample dilution, when NP concentration in complex sample suspensions is already very low and dilution is not possible, other strategies dealing with the problem become necessary.

There are different approaches to surmount non-spectral interferences in ICP-MS, which include different strategies of sample pre-treatment, use of different sample introduction systems, instrument optimization and use of different calibration strategies, such as internal standardization, standard addition, isotope dilution or matrix-matched calibration [19]. Application of these possibilities to SP-ICP-MS is not straightforward in most cases. For instance, internal standardization or isotope dilution would require the simultaneous measurement of two isotopes for a single NP, which is not possible with the sequential instruments most commonly used for SP-ICP-MS (equipped with quadrupole or sector field mass analyzers), at least directly (some alternative methodologies for overcoming this inconvenience and apply isotope dilution have been proposed in the literature [20,21]). The use of matrix matching for SP-ICP-MS, on the other hand, has been studied in some papers where matrix effects have been observed [6,7,22]. Conclusions drawn in these papers were not definitive as to the convenience of such calibration methodology, although no systematic evaluation of the method was performed. However, in a recent publication by Abad-Alvaro and co-workers [23], the benefits of deploying such a calibration strategy have been systematically demonstrated for the determination of AgNPs extracted from biological tissues with TMAH, one of the most popular extraction media for this purpose [24,25].

Although matrix matching could be easy to implement in cases where the matrix composition is well characterized and it is sufficiently simple (e.g., for extraction protocols), application to other situations where the matrix dominating the interfering effects in the ICP-MS instrument is not well known (e.g., environmental samples of unknown composition), or it is very complex, is very challenging. In such situations, the use of the standard addition methodology represents a valuable alternative.

To the best of the authors' knowledge, application of standard addition to SP-ICP-MS has not been reported so far. This may simply be due to the fact that such application is not as immediate as for traditional quantitative analysis. Indeed, it requires some adaptations. In fact, the way in which SP-ICP-MS data are acquired (Transient Acquisition mode, TRA), permits differentiating signals coming from ionic species, which are continuous in time, from those coming from NPs, which provide intense pulses of several hundreds of μs over the continuous signal. This feature has been used in different papers for speciation (ionic *vs.* particulate) analysis [4], but never for calibration purposes. In the same way, NPs of different sizes provide signals that can be distinguished from each other, so that NPs in the sample and NPs added as standards could be differentiated if their sizes were different. Based on these two features, a novel adaptation of the standard addition methodology, aiming at the accurate sizing and counting of NPs in complex matrices *via* SP-ICP-MS has been developed in this work.

Characterization of AuNPs in different complex media was chosen as a model for proofing the concept. For accurate size determination, sample suspensions were doped with ultra-monodisperse AuNPs of known size (less than 5% CV in

diameter). This kind of NPs is expected to be increasingly easy to purchase, according to the evolution of the NP market in the last decade. For accurate determination of the PNC, on the other hand, TE needs to be calculated. For this purpose, sample suspensions also were doped with increasing amounts of Au in ionic form. Application of this calibration strategy to NPs of a different composition (i.e., Ag) was also tested and results are presented.

2. Experimental

2.1. Reagents, standards, and samples

Reagents of analytical purity grade were used for all experiments. Doubly de-ionized water (DDW) (18 MΩ cm) obtained from a Milli-Q water system (Millipore, France) was used throughout for dilutions. 1000 mg L^{-1} Au and Ag stock standard solutions (Inorganic Ventures Inc., USA) were used to prepare the ionic calibration standards. Ionic calibration standards were prepared in 1 mM tri-sodium citrate dihydrate (Merck, Germany).

Several suspensions of nanoparticles with different nominal sizes and chemical compositions were used in this work: 30 nm, 50 nm and 100 nm Ultra Uniform™ AuNPs (less than 5% CV in diameter) were obtained from nanoComposix Europe (Czech Republic); 70 nm, 80 nm and 90 nm AuNPs were obtained from PerkinElmer, USA; 60 nm AgNPs were also obtained from nanoComposix Europe. Reference values for particle number concentration, mass concentration and size distributions of the NP suspensions were provided by the manufacturer (determined by Transmission Electron Microscopy-TEM, and gravimetric analysis) except for the PerkinElmer AuNPs, for which only partial information was available. In this case, analysis by TEM was performed in-home for determination of the average particle size and size distributions. The NP suspensions were vigorously agitated in a vortex for a few minutes before dilution, in order to avoid particle agglomeration. The dilution factors needed for all the NP suspensions to minimize the occurrence of double events during SP-ICP-MS measurements were calculated based on Poisson statistics [13] for a dwell time of 100 μs.

For studying the influence of matrix effects, calibration experiments for the determination of AuNPs prepared in three different media were performed. Particularly, AuNP suspensions were prepared in DDW, 5% (v/v) ethanol/water (prepared from EMSURE® ethanol absolute for analysis, Merck, Germany) and 2.5% (v/v) tetramethylammonium hydroxide (TMAH)/water (prepared from GPR RECTAPUR TMAH 25% in aqueous solution, VWR chemicals BDH®, France). All the samples were stabilized with 1 mM tri-sodium citrate dihydrate.

2.2. Instruments and materials

Two quadrupole-based Inductively Coupled Plasma Mass Spectrometers were used for the measurements: a NexION 300X (PerkinElmer, USA) and a NexION 2000 (PerkinElmer, USA), both equipped with the Syngystix Nano Application module for SP-ICP-MS analysis. Most of the experiments were performed on the NexION 300X, although some additional experiments were carried out with the NexION 2000, which offers a better sensitivity, to confirm that the method could be used for smaller NPs. Instrumental details and operating conditions used with both instruments are summarized in Table 1. Daily performance check and nebulizer gas flow rate were adjusted so that Ce^{++} (70)/Ce^{+} (140) and CeO^{+} (156)/Ce^{+} (140) ratios were equal to or less than 0.03 and 0.025, respectively. Additionally, cross calibration of the counting to analog conversion factor for the detector was daily performed before analyses.

It is worth mentioning at this point that ICP-MS intensities were selected to be obtained in counts instead of counts per second (cps). This is totally optional and similar results should be obtained if cps were selected. The only important question is maintaining the same option for all the experiments performed.

For sample/standard introduction, a T piece designed for internal standard addition manufactured by Elemental Scientific (USA) was used, thus providing an *in situ* standard addition methodology. All NP dilutions were vortexed in a Lab Dancer S040 (IKA®-Werke GmbH & Co. KG, Germany) immediately before their use.

For comparison purposes, the PerkinElmer Au NPs were characterized by TEM. For this purpose, a JEM-1400 TEM instrument (JEOL, USA) at the Central Research Support Services (SCAI) at the University of Málaga was deployed for measuring the particle size distribution.

2.3. Measurement protocol

In order to develop a faster method for performing the standard addition calibration, a split addition model was designed. A T-shaped bifurcation with two flow lines was used for this purpose. The sample containing the target NPs was continuously introduced into the ICP-MS instrument through the main line, using a sampling

Table 1
ICP-MS operation conditions and SP-ICP-MS method parameters.

ICP-MS conditions		
	NexION 300X	NexION 2000
RF power, W	1400	1600
Nebulizer Gas flow, L min^{-1}	0.95	0.98
Plasma Gas flow, L min^{-1}	15	15
Auxiliary gas flow, L min^{-1}	1.2	1.2
Sample introduction system	Glass cyclonic spray chamber-Meinhard Type A concentric quartz nebulizer	Glass cyclonic spray chamber-Meinhard Type C glass nebulizer
Sampler cone	Pt	Ni
Skimmer cone	Pt	Ni
Analyte	Ag, Au	
Mass, amu	107, 197	
Dwell time, μs	100	
Detection mode	Dual (counting + analog)	
NP parameters for calculations		
Density, g cm^{-3}	10.49 (Ag), 19.3 (Au)	
Sample introduction parameters		
Sample uptake rate (Q_1), μL min^{-1}		300
Spike uptake rate (Q_2), μL min^{-1}		70

tube of 0.38 mm ID. For the secondary line, a sampling tube of 0.19 mm ID was used, which provided a flow rate of approximately ¼ of the main one. Through this line, the calibration standards were sequentially mixed with the sample and introduced into the ICP-MS instrument. Under these conditions, a constant and minimal sample dilution was achieved throughout the experiments, which is needed for proper correction of matrix effects. Primary (Q_1) and secondary (Q_2) flow rates were always gravimetrically measured before analysis and varied around 300 and 70 μg L^{-1}, respectively, and hence, a dilution factor of approximately 4.3 was introduced by the T-bifurcation arrangement (Q_1/Q_2). These flows were also measured at the end of each measurement session (lasting, on average, about 1 h) for checking on flow stability, and no significant differences were detected in any of the experiments performed. It is also worth mentioning that all the experimental protocol described in this paper was also repeated with batch additions, and similar values were obtained in all cases.

For each sample analyzed, the following sequence was measured:

1. Sample (line 1) + blank (line 2). Signals for the zero point of both calibration curves and signal for the sample were obtained from this measurement.
2. Sample (line 1) + NP standard (line 2).
3. Sample (line 1) + ionic standard 1 (line 2).
4. Sample (line 1) + ionic standard 2 (line 2).
5. Sample (line 1) + ionic standard 3 (line 2).
6. Sample (line 1) + ionic standard 4 (line 2).

Every point in the sequence was measured in triplicate. The blank solution used in point 1 was prepared with 1 mM tri-sodium citrate dihydrate in DDW. A schematic representation of the sample introduction system and the measuring protocol developed for standard addition calibration is displayed in Fig. 1.

For proofing the concept of standard addition calibration, experiments in the different matrices tested were conducted using a 50 nm AuNPs suspension as the sample, a suspension of 100 nm Ultra Uniform™ AuNPs as NP standard, and four Au (III) solutions of 4.3, 8.6, 12.9 and 17.2 μg L^{-1} as standards for ionic calibrations. These concentrations were calculated considering the dilution factor introduced by the T-shaped bifurcation arrangement (Q_1/Q_2) and in order to achieve a final concentration in the measured sample of 1–4 μg L^{-1}.

Additionally, the TE determined with Au standards was also used for analysis of samples containing Ag NPs. In such case, the measurement sequence was modified. For determination of the TE, points 2–6 in the sequence were measured for *m/z* 197 (Au), using the same standards mentioned above. Then, points 1 and 3–6 in the sequence were measured again for *m/z* 107 (Ag). In this case, a suspension of 60 nm Ag NPs was used as the sample, while aqueous solutions of this element in the same range as used for Au (1–4 μg L^{-1} in the measured sample, points 3–6) were deployed for ionic calibration.

For comparison purposes, measurements were also carried out by using external calibration with ionic matrix-matched standards. In this case, the T piece was also deployed to compare results using the same sample introduction system. The sample was measured in exactly the same way as for standard addition calibration (point 1 in the sequence above), but calibration standards were measured differently. In particular, a blank solution (corresponding to one of the three matrices investigated) was introduced through line 1 instead of the sample and the standards were introduced through line 2. In this case, an additional point was measured to determine the zero point of the calibration curves: blank (matrix solution) through line 1 + blank (1 mM tri-sodium citrate dihydrate solution in DDW) through line 2.

For characterization of the PE AuNP samples by TEM, on the other hand, 10 μL of each stock AuNP suspension (approximately 0.05 mg mL^{-1}) were deposited onto carbon grids and let dry for at least 1 h. Subsequently, the grids were observed by TEM and scanned for taking pictures of the deposited NPs. A minimum of ten pictures were taken for each sample analyzed to count at least 200 different NPs. Next, the pictures were manually processed with the software ImageJ, where the diameter of each NP was measured by using the respective scale. The full process requires a considerable amount of work (at least 1 h of TEM measurements and 1 h of

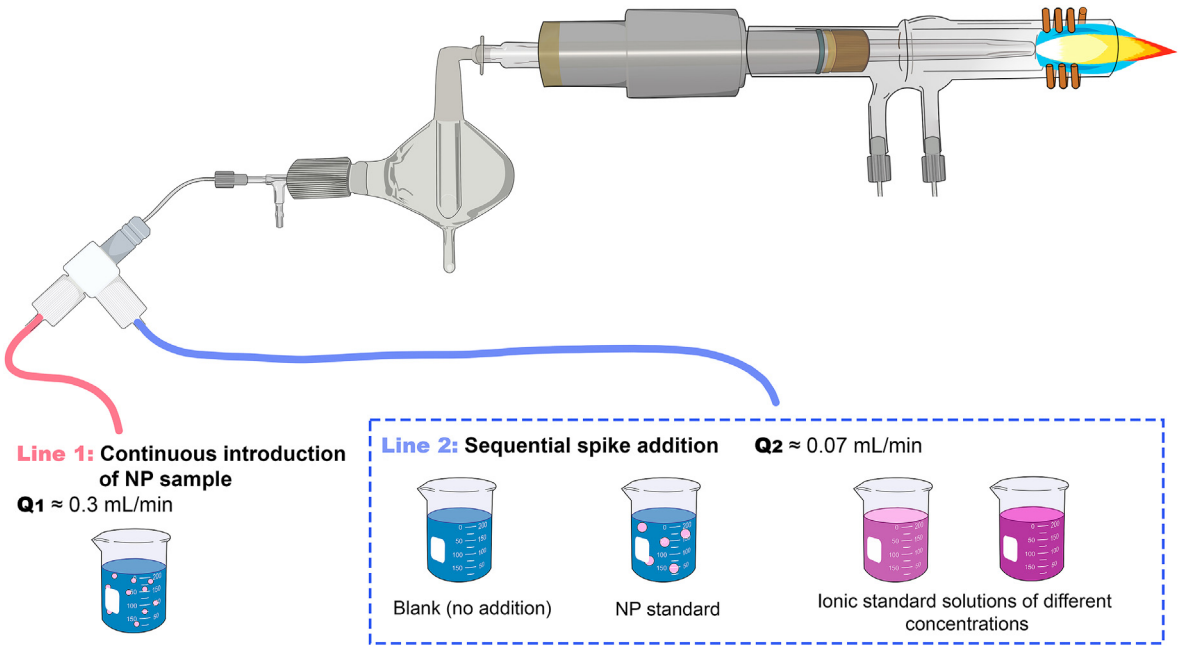

Fig. 1. Sample introduction system for standard addition calibration by SP-ICP-MS.

computer processing per sample), concentrated samples (the stock solutions were used) and only provides an estimation of the average NP size distribution (NP number concentration cannot be obtained by this technique). By comparison, SP-ICP-MS measurements are able to count about 1000 NPs in only 60 s for samples prepared in high dilutions, leading to an estimation of both size distribution and particle number concentration.

2.4. SP-ICP-MS data processing

All ICP-MS data was acquired with the PerkinElmer Nano Application module of the NexION ICP-MS Syngistix software (*version 2.1.*). When dwell times in the μs range are used, each NP pulse (known to have a duration around 300–500 μs) is composed of several events, and hence, the raw data (time vs. counts) provided by the software needs to be further processed for recognizing and summing the signals for each NP. To this end, an in-house developed script written in GNU Octave was used in this case, which fundamentals are illustrated in Fig. 2. This script is based on an algorithm that searches for maximum and minimum datapoints to identify NP signals as peaks over the continuous background (BG). For this purpose, a smoothing function is first applied to the raw data to minimize the influence of possible signal fluctuations. Next, signals coming from one NP are identified as peaks circumscribed between two consecutive minima with a maximum in the middle, which intensity must be over a manually inputted threshold. The value for this threshold is calculated by filtering the full raw data set iteratively with the 5s criterion. The script also includes a second threshold and an algorithm for recognizing double events (signals coming from two overlapping NPs), although its use is unnecessary if sample dilutions are properly selected as commented on in section 2.1 and, thus, this feature is not further discussed herein for the sake of simplicity.

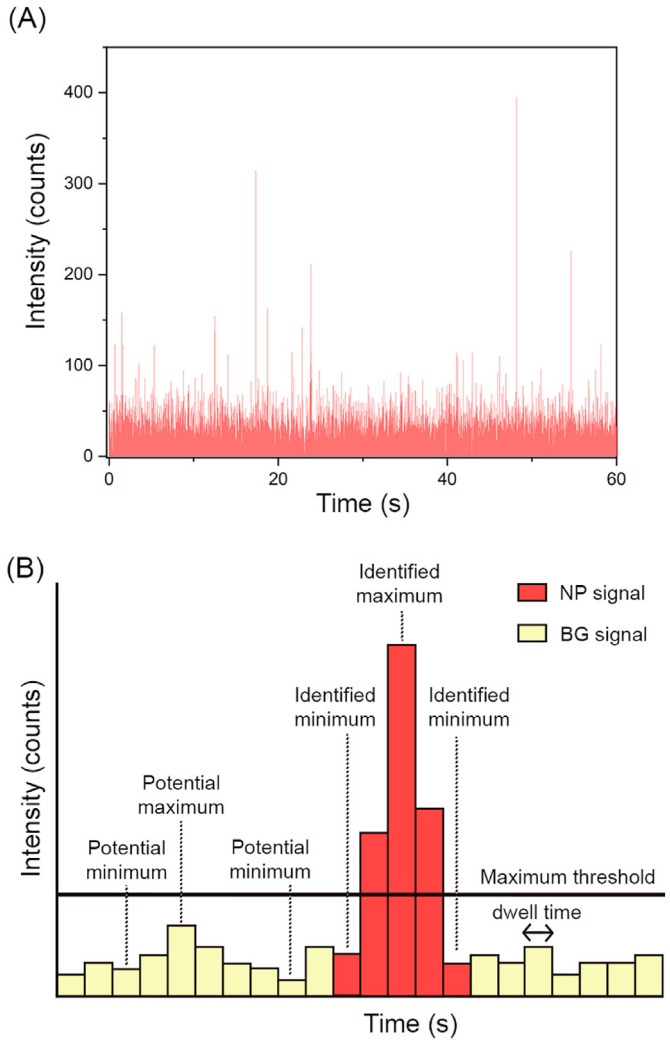

Fig. 2. (A) Example of TRA raw data obtained by SP-ICP-MS. (B) Parameters of the GNU-Octave in house developed script for identification of NP and Background signals. Only peaks with its maximum over the maximum threshold (defined using the 5σ criterion on the raw data) are counted as NPs. The magnitude of the signals included in (B) has been altered for the sake of clarity.

Datapoints not identified as belonging to any NP are considered as BG, such that the script can calculate the average BG signal and subtract it from each datapoint identified as NP. Finally, datapoints identified as belonging to one NP, once BG corrected, are summed up to provide the net signal for each NP. The output signal consists of a time column with a point every 100 μs (or the dwell time selected if is different from this value) and a column with the net signals for each NP. The total signal calculated for each NP is left in the first cell of all of those summed and the rest of them are left empty. The script also permits to visualize the signals identified as BG next to the NP signals. Microsoft Excel (Redmond, Washington, USA) and OriginPro (OriginLab, Northampton, MA, USA) were further used for calculations and graphical representations.

For particle size calculations, two methods were tested and compared in this work. First, the ICP-MS response for the NPs in counts fg^{-1} was directly calculated by constructing a calibration curve with NPs of known size. As indicated before, a suspension of 100 nm Ultra Uniform™ AuNPs was used as NP standard for this purpose. With this method (referred to as particle calibration from now on), the mass (fg) of each detected NP ($m_{NP,PC}$) can be calculated according to equation (1), where I_{NP} is the net intensity recorded for each NP (the particle signal intensity minus average baseline intensity in counts) and S_{NP} is the slope of the calibration curve with NPs of known size (counts fg^{-1}).

The second method consists on measuring the ICP-MS response in counts $L\mu g^{-1}$ (by constructing a calibration curve with ionic standards of known concentration for the analyte of interest) plus determining the transport efficiency (TE), which was calculated using the size calibration method described by Pace et *al.* [12] In this method, the transport efficiency is obtained as the ratio of the ionic and nanoparticular calibration slopes, both expressed in counts fg^{-1} of analyte introduced into the ICP-MS instrument. According to this method, the TE was calculated following equation (2), where S_{ion} is the slope of the calibration curve with ionic standards (counts L μg^{-1}; for calculation of this slope, the final concentrations reaching the ICP-MS instrument of 1–4 $\mu g\ L^{-1}$ were considered), Q_1 is the sample flow rate introduced in the ICP-MS instrument through line 1 ($\mu L\ min^{-1}$), t_{dwell} is the dwell time (s) and 60 is the conversion factor from minutes to seconds. Additionally, the mass (fg) for each NP detected with this method (referred to as ionic calibration from now on) ($m_{NP,IC}$) can be calculated *via* equation (3).

The diameter (nm) of each unknown particle detected (d_{NP}) was subsequently calculated according to equation (4), where m_{NP} refers to the mass of each detected NP calculated according to either equation (1) or equation (3) (fg), while ρ is the known density of the targeted particle ($g\ cm^{-3}$). For this parameter, values included in Table 1 were used for the different NPs analyzed.

Finally, the number of NPs per mL in the sample analyzed, the so-called particle number concentration (PNC), was calculated according to equation (5), where N is the total number of particles detected during one replicate measurement, t_{acq} is the acquisition time of one replicate measurement (min), and TE is the transport

efficiency previously determined according to equation (2).

$$m_{NP,PC} = \frac{I_{NP}}{S_{NP}} \quad (1)$$

$$TE = \frac{\frac{S_{ion}}{Q_1 \cdot (t_{dwell}/60)}}{S_{NP}} \cdot 10^{-3} \quad (2)$$

$$m_{NP,IC} = \frac{I_{NP} \cdot \frac{t_{dwell} \cdot Q_1}{60} \cdot TE}{S_{ion}} \quad (3)$$

$$d_{NP} = \sqrt[3]{\frac{6 \cdot m_{NP}}{\pi \cdot \rho}} \cdot 10^2 \quad (4)$$

$$PNC = \frac{\frac{N}{Q_1 \cdot t_{acq}}}{TE} \cdot 10^3 \quad (5)$$

As seen from equations (1)–(5), the calculations for determining the size and PNC of the NP samples are the usual ones for SP-ICP-MS when external calibration is performed. The main difference in the standard addition approach regarding data processing is related with the extraction of data for performing these calculations. As described in section 2.3, the ionic calibration curve is measured by doping the NP samples with ionic standards of different concentrations (points 3 to 6 in the measuring sequence described in section 2.3), and so, ionic and NP signals are mixed in the raw data. In the same way, the NP calibration curve is measured by doping the NP samples with other NPs of similar composition and known size (point 2 in the measuring sequence described in section 2.3), so that frequency/signal histograms show mixtures of size distributions. To extract the data from these mixed signals, OriginPro software was used. In particular, every calibrating histogram (either the ionic signal or the doping Ultra Uniform™ NPs) was adjusted with OriginPro to a Gaussian fit, and the average value (in counts) predicted by the program (X_c) was used to construct the calibration curves and to determine the parameters needed for calculations (S_{NP}, S_{ion}, and TE). These parameters were finally used in the sample replicates (point 1 in the measuring sequence described in section 2.3) to calculate the NP size and PNC by using equations (1)–(5). An example of the mixed signal distributions obtained in this work for the case of AuNPs, as well as a summary of data processing and calculations performed, is included in Fig. 3. More details on selection of the ionic and NP doping concentrations and sizes, respectively, as well as data processing with OriginPro software are provided in section 3.

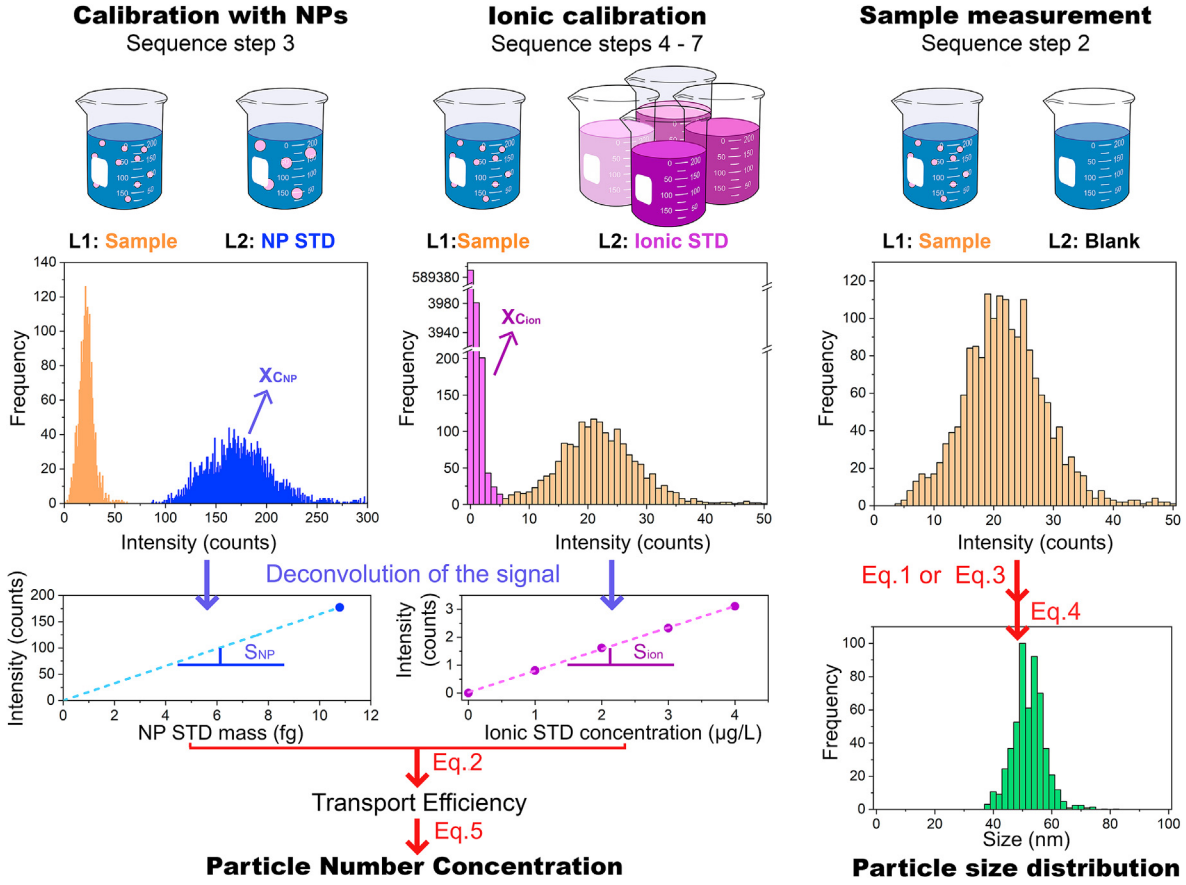

Fig. 3. Mixed signal distributions obtained with the standard addition method developed and data processing for SP-ICP-MS. First frequency *vs.* intensity figure on the upper left side (calibration with NPs) represents a mixture of AuNPs of 50 nm (sample, orange) and 100 nm (standard, blue). In the rest of the frequency *vs.* intensity figures the signal for the sample (50 nm AuNPs, orange) is either mixed with an ionic standard (middle figure, pink signal) or alone (right figure). After application of equation (1) or (3) and (4) the sample signal is converted to a particle size distribution histogram (bottom right figure, green bars). (For interpretation of the references to colour in this figure legend, the reader is referred to the Web version of this article.)

3. Results and discussion

3.1. Particle size calibration with NP standards

3.1.1. Linearity of calibration plots with NP standards and influence of the matrix

Calibration of SP-ICP-MS with NPs of known size has been considered superior to calibration with ionic standards [26], as it is not necessary to assume that the signal generated by the analyte in NP form is similar to that of the analyte in ionic form, once the transport efficiency is corrected for. However, this strategy has been much less frequently used than calibration with ionic standards, most likely due to the lack of well-characterized and monodisperse NP standards. Due to the fast-growing NP market seen in the last decade, this kind of NPs is starting to be commercially available and expected to be increasingly easy to purchase. In this work, a set of Au Ultra Uniform™ standards of different sizes, with a high degree of monodispersity (less than 5% CV in size), was studied for calibration with the standard addition methodology. With such a high monodispersity, average counts per analyte mass can be accurately determined. The size distributions obtained by SP-ICP-MS adjust well to a Gaussian fit centered at the nominal mass.

The first question to be considered for selecting a NP standard for calibration is the linearity of the ICP-MS response for NPs of different sizes. It has been shown in the literature that calibration plots with NPs of different sizes can lose linearity at high NP masses due to different factors, two of which have been identified as the most serious [26]. First, the linear dynamic range of electron multipliers operated in pulse counting mode is limited, although this problem can be easily solved by working in dual detection (analog + counting modes) and cross calibrating the detector at the beginning of the experiments. Second, different degrees of vaporization/ionization for the particles of different sizes may be observed, in which case specific optimization of the measuring conditions for SP-ICP-MS (forward power and sample gas flow rate) might be needed [13,26].

In this work, linearity of the calibration plots obtained for NPs of 30 nm (Nexion 2000 only), 50 and 100 nm diameter (plus the blank measured in sequence point 1) was studied. Experiments proved that calibration curves in that mass range and for the experimental conditions used showed an excellent linearity ($R^2 \geq 0.999$; see an example calibration curve in Fig. S1 included in the supplementary material), provided that cross-calibration of the detector was performed at the beginning of each working session. As a result, any of the NP standards tested could be used for calibration in the mass range selected. For proofing the concept, the 100 nm Au NPs were selected as one-point NP standard for size calibration of smaller Au NPs. In most of the experiments, 50 nm Au NPs were used as the target sample.

To show that this one-point calibration was feasible, the slopes obtained for the calibration plots with several points (blank plus Au NPs of 30 -NexION 2000 only-, 50 and 100 nm) and calibrating with only one point (blank plus Au 100 nm) were compared in the different media subjected to study (DDW, 5% Ethanol, 2.5% TMAH). Results obtained with the NexION 300X instrument are shown in Table 2. As seen from these data, no significant differences were observed between the slopes with one point (100 nm AuNP) or with several points (50 and 100 nm AuNPs) in any of the tested media, according to a paired *t*-test at a 95% confidence level ($t_{calculated} = 1$ and $t_{tabulated} = 4.30$).

Moreover, it is shown in this table that sensitivity changes depending on the sample matrix, especially for the case of ethanol (significant differences were observed for slopes measured in TMAH and ethanol media with respect to the slope in DDW according to t-tests). It seems from these data that a method capable of compensating for potential matrix effects when complex samples are analyzed would be very valuable for accurate results to be obtained, even when calibration with NP standards is carried out. Although data shown in Table 2 were obtained with the Nexion 300X ICP-MS instrument, similar results were observed for the Nexion 2000 ICP-MS instrument.

Table 2
Comparison of the slopes obtained for calibration with NP standards of different sizes in the Nexion 300X instrument. 1 point calibration slope refers to calibration with 100 nm AuNP only, while 2 points calibration slope refers to calibration with 50 nm and 100 nm AuNP. In both cases, a blank was also measured (sequence point 1) and used to build the calibration curve. Confidence intervals are given as ± one standard deviation of three replicate measurements of the slopes.

Medium	1 point calibration slope (counts fg^{-1})	2 points calibration slope (counts fg^{-1})
DDW	16.4 ± 0.5	16.4 ± 0.5
5% Ethanol	21.9 ± 0.1	21.9 ± 0.1
2.5% TMAH	18.1 ± 0.1	18.0 ± 0.1

3.1.2. Size of the NP standard with respect to the NP sample

As shown in section 2.4, the standard addition method proposed provides mixed size distributions for the NP standard and the NPs in the sample. In the example shown in Fig. 3, the two NP size distributions (that of the sample-50 nm AuNP and that of the standard-100 nm AuNP) are completely resolved. In such case, determination of the average value in counts fg^{-1} for the standard (X_c) can be accurately performed by simply averaging the signals corresponding to the second peak of the histogram. However, obtaining this perfect resolution might not be easy in real samples.

To test the influence of the size of the NP standard used for calibration with respect to the size distribution of the NP sample, the following experiments were conducted. Three AuNP suspensions in DDW medium of 70 nm, 80 nm, and 90 nm, respectively, were analyzed for particle size using the 100 nm Ultra Uniform AuNP as standard. Histograms obtained in these cases showed closer populations for the sample NP and the standard, with the extreme situation of the 90 nm sample for which it was difficult to distinguish the two populations in the mixed histogram, as shown in Fig. 4B.

Although the situation might seem complex to solve, it is important to remember that the only data necessary for calibration is the X_c value (i.e., the most frequent intensity value for the 100 nm AuNP standard). Moreover, the size distribution for the sample alone has already been determined (measured in point 1 of the measuring protocol and depicted in Fig. 4A), which is a crucial factor, and the size distribution of the standard (selected to be monodisperse) adjusts well to a Gaussian peak, as discussed before. Thus, the X_c value can be obtained by performing a mathematical deconvolution, which would be hardly reliable without these *a priori* conditions. OriginPro software was used for this purpose. As shown in Fig. 4A for the 90 nm AuNPs sample, a mathematical model describing the sample size distribution can be obtained with this software. In this case, a Gaussian distribution was selected as model, although other peak modelling options are available in case different sample distributions are obtained. Afterwards, the relevant model parameters (*i.e.,* average: X_c, area: A, and full width at half maximum: FWHM, in this case) can be used for deconvoluting the mixed distribution, which will return a Gaussian model for the distribution of the NP standard. Finally, the average value for the standard (Xc_2) can be obtained from the Gaussian model.

Average X_c values obtained for the 100 nm NP standard, isolated and mixed with the 70, 80 and 90 nm AuNPs in DDW water, are shown in Table 3. As seen in this table, the X_c value for the 100 nm

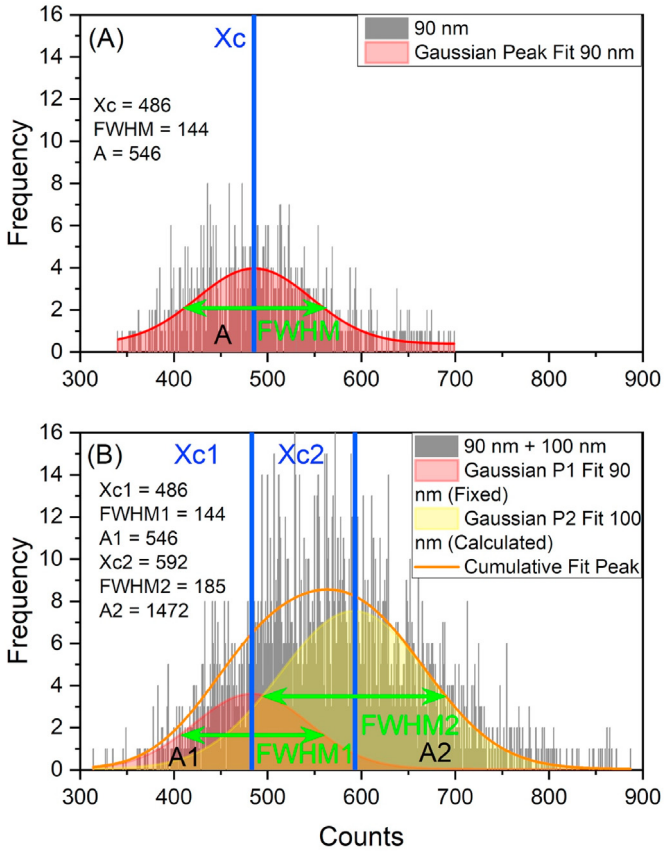

Fig. 4. Signal deconvolution for a mixed distribution of 90 nm AuNPs (sample) and 100 nm AuNPs (standard). (A) 90 nm AuNP distribution and Gaussian fit parameters obtained with OriginPro software. (B) 90 nm + 100 nm AuNPs mixed size distribution deconvoluted with OriginPro software. Xc1, FWHM1 and A1 parameters were fixed as obtained in the model shown in Fig. 4A.

AuNP standard is similar in all cases, proving that the deconvolution method works properly. Moreover, the size determined for the different samples analyzed with the PC method (also shown in this table) agrees well with the expected values determined by TEM.

3.2. Size and particle number calibration with ionic standards

As shown in equation (5), determination of the PNC by SP-ICP-MS requires the determination of the transport efficiency (TE). As described in detail in section 2.4, determination of this parameter was carried out by the particle size method [12], which has been reported to be more robust than the particle frequency method as it is not affected by NP losses to the container walls [27]. This method requires measuring a calibration curve with ionic standards of known concentration for the analyte of interest, in addition to the calibration curve with NPs measured as described in section 3.1. The transport efficiency is then obtained as the ratio of the ionic and nanoparticular calibration slopes (both expressed in counts fg^{-1} of analyte introduced into the ICP-MS instrument) previously measured. Average ionic slopes (S_{ion}) for a set of Au standards in the range 1–4 μg L^{-1} (once taken into account the dilution factor introduced by the T-shaped bifurcation arrangement; all the concentrations of ionic standards will be given in the same way from now on) and TE values obtained for the different media tested, with external calibration with ionic matrix-matched standards and the standard addition method, respectively, are gathered and compared in Table 4. For both parameters, no significant differences were observed between the values obtained with both calibration methods in any of the tested media, according to a paired *t*-test at a 95% confidence level. On the other hand, and as could be anticipated, different TE values were obtained when the samples were dispersed in ethanol or TMAH when compared to DDW media. These differences are especially important in the case of the ethanol matrix, meaning that a PNC biased high by *ca.* 25% would have been obtained if the TE value determined in DDW would have been used.

The ICP-MS response (S_{ion}) and the TE can also be used for calibrating the particle size using equations (2)–(4) shown in section 2.4, which should provide similar values to those obtained by direct calibration with NP standards (equation (1)) considering that the particle size method was used for calculating the TE (see section 3.3 for the data). Again, as derived from data included in Table 4, calibration of samples in TMAH or ethanol matrices with standards in DDW would lead to size results biased high (as calculated size depends on the ratio TE/S_{ion}), especially for the ethanol matrix, proving the need for methods capable of compensating for matrix effects.

Alternatively, and in cases where reference NPs were not available, the standard addition calibration with ionic standards could be performed by measuring the ionic calibration curve as indicated in section 2.4 and introducing the TE value determined by other means [12,28] in equations (3) and (4). This is an important aspect to keep in mind, as it means that a standard addition approach can be used even in the absence of highly monodispersed and reliably characterized NP suspensions.

As for selection of concentration for the standards, it needs to be reminded that calibration of NPs with ionic standards is normally carried out by extrapolation. In fact, ICP-MS signal intensities measured for NPs of different sizes increase to the cubic power with NP diameter, such that, for instance, measuring AuNPs with the Nexion 2000 in the range of 30–100 nm diameter implies measuring ICP-MS signal intensities in the range of several thousands to several millions of counts per second. In spite of this fact, calibration standards are normally selected in the low range of concentrations, taking advantage of the large dynamic range of ICP-MS spectrometers (if the detector is adequately cross-calibrated), so that calibration of NPs is performed by extrapolation and potential contamination or memory effects due to an excessively high concentration of ionic standards is avoided. According to the ISO guideline ISO/TS 19590, a range in the 1–5 μg L^{-1} for ionic (external) calibration standards is considered a good starting point for calibration of NPs [29].

Table 3
Results for the analysis of AuNPs samples of different sizes in DDW with the particle calibration (PC) method. X_c refers to the average values obtained for the 100 nm AuNP standard following the deconvolution method described in Fig. 4. Confidence intervals are given as ± one standard deviation of three replicate measurements.

Sample	X_c (AuNP 100 nm)	Size (nm) determined with PC Method	Reference size (TEM) (nm)[a]
Blank	595 ± 8	–	–
Au 70 nm	598 ± 5	75.4 ± 0.4	74.0 ± 7.0
Au 80 nm	589 ± 6	78.1 ± 0.5	77.9 ± 5.3
Au 90 nm	589 ± 7	98.5 ± 0.3	95.5 ± 5.3

[a] TEM deviations represent dispersity of the NP distribution as determined by TEM, and are not directly comparable with the calculated deviations of the mean presented in this table for our method.

Table 4
Average ionic calibration slopes for a set of Au ionic standards in the range 1–4 μg L^{-1} (S_{ion}) and TE values obtained by the particle size method in the different media tested. Confidence intervals are given as ± one standard deviation of three replicate measurements.

Medium	% TE (EXT)	% TE (S-ADD)	S_{ion} (EXT) (counts L μg^{-1})	S_{ion} (S-ADD) (counts L μg^{-1})
DDW	9.4 ± 0.3	9.6 ± 0.3	0.772 ± 0.008	0.792 ± 0.002
5% Ethanol	12.9 ± 0.1	13.0 ± 0.1	1.42 ± 0.01	1.43 ± 0.02
2.5% TMAH	9.0 ± 0.3	8.9 ± 0.1	0.82 ± 0.03	0.81 ± 0.01

In the particular case of the standard addition method proposed in this work, determination of the ionic standard average intensity (X_c) needed for constructing the calibration curves is performed in the mixed histograms shown in Fig. 3. Under these circumstances, concentration for the standards is preferably selected to give a signal intensity (per event) clearly distinguishable (smaller) from that of the NP signal, as this will provide a more accurate determination of the X_c value. In this case, and for the Nexion 300X instrument, the set of ionic standards selected in the range of 1–4 μg L^{-1} provided average signal intensities in the range of 10^3–10^4 cps. The Au NPs (50–100 nm), on the other hand, provided average signal intensities in the range of 10^5–10^6 cps. Again, it is important to work in dual detection mode (counting + analog) and cross-calibrate the detector at the beginning of the experiments for ensuring a linear response in the range of the signals recorded.

3.3. Results

To test the validity of the method designed, the 50 nm AuNPs Ultra Uniform™ sample was dispersed into the three different matrices under study that were subsequently analyzed with the standard addition methodology. Results obtained in each of the matrices are gathered in Table 5. For comparison purposes, results obtained with external calibration using ionic matrix-matched standards are also included in this table. As seen in the table, average sizes obtained for the 50 nm AuNPs Ultra Uniform™ sample with the three different calibration strategies tested (i.e., the direct calibration with the spiked NP standard, external calibration with ionic matrix-matched standards and calibration with spiked ionic standards) are very similar to the reference value, regardless of the matrix.

Validation of the PNC is more troublesome. First, and to the best of our knowledge, there is no reference material commercially available for NP number concentration. On the other hand, information included in most of the certificates of analysis for commercial NPs is usually a calculated value from the total analyte concentration values (normally obtained by ICP-MS) and the average NP size (obtained by TEM). Thus, it is not obtained by a method fully independent from ICP-MS measurements. Finally, the lack of stability of NP suspensions makes this value to be potentially affected by time. As a consequence, validation of the standard addition methodology for determination of PNC was performed by comparing the PNC values obtained for each sample using the standard addition method and the external calibration with matrix-matched standards, respectively, the latter being considered as the best current reference for SP-ICP-MS, providing the matrix is known in advance.

Results were expressed as percentage recovery and are also included in Table 5. As seen from this table, recoveries close to 100% were obtained in all cases, as expected by the very similar TE values obtained with both calibration methods and shown in Table 4. This proves that the standard addition method and the processing of the signals in the mixed histograms do not introduce significant bias in the determined PNC.

Finally, Fig. 5 presents the NP size distributions for the 50 nm AuNP suspensions in the three media tested and obtained with the standard addition calibration method with the spiked NP standard. The size distributions obtained with the other calibration methods (external calibration with ionic matrix-matched standards and standard addition with ionic aqueous standards) are obviously very similar (it has to be reminded herein that the sample alone is measured exactly in the same way for the three calibration methods) and have not been included for simplicity. As seen in this figure (and besides the close average values shown in Table 5) similar size distributions were obtained with these calibration methods in all media tested, which we have quantified by comparing the full width at half maximum (FWHM) of the Gaussian fitting obtained with OriginPro software (average values included in the figure). This further proves that the standard addition method is able to accurately correct for matrix effects and does not induce any additional bias compared to the traditional external calibration with matrix-matched standards methodology.

These FWHM values are directly comparable to the polydispersity values provided by the manufacturer (which are given as one standard deviation of the size values obtained by TEM). For the 50 nm AuNPs analyzed, the reference value is 50.3 ± 2.3 nm, which, assuming a Gaussian distribution, would correspond to a FWHM of 5.42 nm. As seen in Fig. 5, values obtained by SP-ICP-MS are larger than those obtained by TEM by a factor of almost 2. This circumstance could be due to sample stability issues and/or be inherent to the SP-ICP-MS methodology. As will be shown in the next section, results obtained for a AgNP suspension follow a different trend, pointing to an effect related to the stability of the AuNPs measured.

Overall, results indicate that the standard addition method proposed is a valid means for dealing with matrix effects in the characterization of NPs in complex matrices. This methodology

Table 5
Results for the analysis of 50 nm AuNPs dispersed in different matrices and using the different calibration methods described in the paper. For standard addition calibration with NP standards, the 100 nm AuNP Ultra Uniform™ standard was deployed. Confidence intervals are given as ± one standard deviation of three replicate measurements.

Medium	Size (nm)*			PNC
	External calibration	Standard addition		% Recovery S-ADD/EXT
	Ionic matrix-matched standards	Ionic standards	NP standards	
DDW	51.1 ± 0.1	51.2 ± 0.1	51.2 ± 0.1	97.0
5% Ethanol	49.7 ± 0.1	49.7 ± 0.1	49.7 ± 0.1	98.9
2.5% TMAH	52.0 ± 0.1	52.0 ± 0.1	51.0 ± 0.1	101.5

*Reference size provided by the manufacturer: Au (50.3 ± 2.3 nm). This reference deviation represents the dispersity of the NP distribution and is not directly comparable with the calculated deviations of the mean presented in this table for our method. Comments on measured dispersity values are provided in Fig. 5.

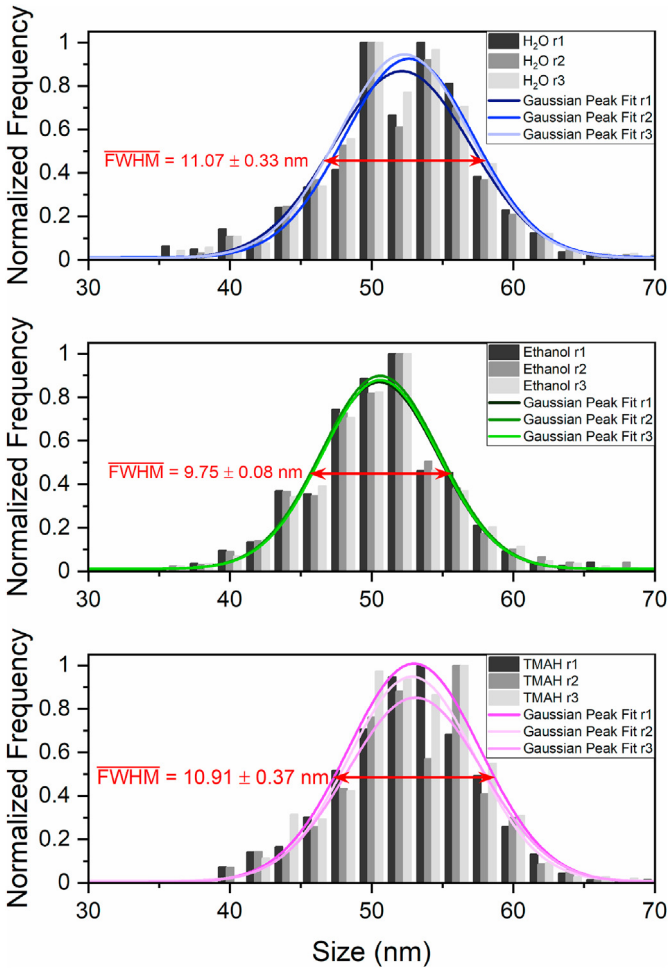

Fig. 5. Particle size distributions obtained for the 50 nm AuNP sample dispersed in the three different matrices tested and analyzed with the standard addition methods and calibration with NP standards. Three different replicates (r1, r2 and r3) are depicted for each distribution. Average FWHM values obtained with a Gaussian fit are presented in the figures for comparison purposes.

would be especially indicated in the cases where the nature of the sample matrix is not fully known thus precluding preparation and use of matrix-matched standards.

3.4. Analysis of NPs of different chemical composition (Ag)

Finally, the possibility of characterizing NPs of different chemical composition (for which NP standards are not available) was intended, deploying the TE value determined with Au NPs for calculations, as the TE should not depend on the chemical composition of the particulate material. For checking this possibility, an Ag NPs suspension of 60 nm nominal diameter was prepared in DDW (also stabilized with 1 mM tri-sodium citrate dihydrate), and calibration with the standard addition methodology (ionic calibration) was carried out.

First, the TE was calculated using the particle size method with Au NPs. For this purpose, the Ag sample was sequentially doped with 100 nm Au NPs and Au (III) standards (1–4 μg L^{-1}) and was analyzed for *m/z* 197 (Au), following the measurement protocol described in section 2.4. The TE was subsequently calculated using equation (2). Next, the sample was doped with a series of Ag ionic standards (1–4 μg L^{-1}) and was analyzed for *m/z* 107 (Ag). NP mass and diameter were subsequently calculated following equations (3) and (4).

Table 6
Results for the analysis of 60 nm AgNPs dispersed in DDW and using external and standard addition (ionic standards) calibration methods. Confidence intervals are calculated as ± one standard deviation of three replicate measurements.

	Average size (S-ADD)	Reference size (TEM)[a]	% TE
Ag 60 nm	62.4 ± 0.2	59 ± 6	6.34 ± 0.05

[a] The reference deviation represents the dispersity of the NP distribution and is not directly comparable with the calculated deviations of the mean presented in this table for our method. Comments on measured dispersity values are provided in Fig. 6.

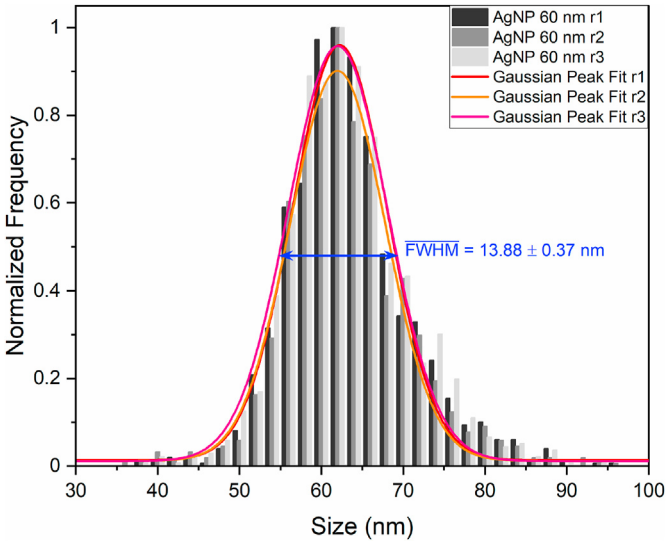

Fig. 6. Particle size distributions obtained for a 60 nm AgNP sample dispersed in DDW with the standard addition method using AuNPs for determination of the TE. Three different replicates (r1, r2 and r3) are depicted for the distribution. Average FWHM value obtained with a Gaussian fit is presented in the figure.

Results for these determinations are included in Table 6. As seen from this table, average size values obtained with the standard addition methodology are comparable to the reference size value provided by the manufacturer. As for the TE, the value obtained in this case is significantly lower than values presented in Table 4 due to the fact that measurements were carried out in a different instrument (Nexion 2000) with a different sample introduction system (see Table 1). The good results obtained for the sizing of the NPs, though, indicate that this value is accurate.

Particle size distribution for the AgNP suspension along with FWHM is also shown in Fig. 6. The reference value provided by the manufacturer in this case is 59 ± 6 nm, where the confidence interval is given as one standard deviation of the size distribution obtained by TEM. Assuming a Gaussian distribution, this standard deviation would correspond to a FWHM value of 14.1 nm, which is in close agreement with the value obtained by SP-ICP-MS shown in Fig. 6. As discussed before, this is a different trend to that observed for AuNPs and presented in section 3.3, which seem to suggest problems with stability of the AuNP samples subjected to analysis and/or inaccuracies in the reference values provided by the manufacturer, rather than factors related to the SP-ICP-MS technique itself. This question, however, should require further specific investigation, which is out of the scope of this paper.

The key conclusion of this section is that the TE can be determined with any available NPs (or by other methods based on estimating the amount of sample aspirated and the waste [12,28]) and the standard addition can be deployed using ionic aqueous standards of the target element. In other words, the approach

proposed enables accurate estimation of both the size and PNC of NPs of other composition than those used to estimate the TE, and thus can be considered as a universal approach for the characterization of metallic NPs.

3.5. Conclusions

In this paper, a standard addition methodology for the characterization of NPs by SP-ICPMS, capable of compensating for matrix effects in complex matrices is presented. The use of a T-shaped bifurcation designed for internal standard addition allows for fast addition experiments with constant and minimal sample dilution. Size determination can be rapidly performed by simple addition of a single NP standard of the same target NP and of known size. Accurate results are obtained with this method in matrices showing matrix effects, provided that (i) ICP-MS measurements are carried out in dual detection mode and cross calibration is performed at the beginning of the working session for ensuring linear response for the samples analyzed; and (ii) signal deconvolution is performed in the case that the sample analyzed and the NP standard show overlapping size distributions.

As for PNC determination, TE determination is also needed and can be performed by additionally measuring a calibration curve with ionic standards sequentially added to the measured sample. With these values, calibration of the sensitivity with ionic standards (instead of using the NP standard) is also possible and provides accurate size values and comparable PNC as those obtained by external calibration with ionic matrix-matched standards. In principle, and according to these results, size and PNC determination could be also performed by only measuring the ionic standards and using the TE determined by other means.

Finally, also NPs of other types for which no NP standard is available can be analyzed. In such case, the TE is determined using a NP standard of a different element (Au is recommended as highly monodisperse suspensions of known size are available) and ionic solutions of the same element, while the sensitivity is calculated with ionic standards of the target element, present in the NP of interest.

The method provides a valuable alternative for characterization of NPs in complex samples where the matrix characteristics cannot be fully mimicked to apply matrix-matched calibration and/or when dilution of the sample is not recommended.

In terms of sample throughput, the method requires more measurements than an external approach if the TE needs to be determined for every sample monitored. However, that may not be a very frequent case in real labs where assuming that TE efficiency is the same for a type of sample (e.g., a type of biological fluid) may be a valid solution for faster results, while of course using the full approach will guarantee more accurate results.

Overall, the approach proposed offers flexibility, so it can be adapted to different situations.

CRediT authorship contribution statement

Maite Aramendía: Conceptualization, Methodology, Supervision, Writing – original draft, Writing – review & editing. **Juan Carlos García-Mesa:** Data curation, Investigation, Methodology, Validation, Writing – original draft, Writing – review & editing. **Elisa Vereda Alonso:** Funding acquisition, Data curation, Writing – review & editing. **Raúl Garde:** Data curation, Visualization, Writing – review & editing. **Antonio Bazo:** Visualization, Writing – review & editing. **Javier Resano:** Software, Writing – review & editing. **Martín Resano:** Conceptualization, Funding acquisition, Methodology, Project administration, Supervision, Writing – review & editing.

Declaration of competing interest

The authors declare that they have no known competing financial interests or personal relationships that could have appeared to influence the work reported in this paper.

Acknowledgements

The funding obtained by Grant PGC2018-093753-B-I00, funded by MCIU/AEI/10.13039/501100011033 and by "ERDF A way of making Europe", and by the Aragón Government (Construyendo Europa desde Aragón, Grupo E43_20R) is acknowledged. This work was also supported by MCIU/AEI/ERDF (EU) (grant PID2019-105660RB-C21/AEI/10.13039/501100011033) and by the Aragón Government (T5820R research group). Finally, the funding obtained by Project UMA18FEDERJA060 from the Junta de Andalucía is also acknowledged. A. Bazo thanks the Aragón Government for his doctoral grant.

Geoff Coleman from Meinhard®-Elemental Scientific glass-blowing is thanked for kindly providing the pieces for adapting the T-piece to our nebulizer.

Appendix A. Supplementary data

Supplementary data to this article can be found online at https://doi.org/10.1016/j.aca.2022.339738.

References

[1] F. Laborda, E. Bolea, J. Jiménez-Lamana, Single particle inductively coupled plasma mass spectrometry: a powerful tool for nanoanalysis, Anal. Chem. 86 (2014) 2270–2278, https://doi.org/10.1021/ac402980q.

[2] P. Krystek, A. Ulrich, C.C. Garcia, S. Manohar, R. Ritsema, Application of plasma spectrometry for the analysis of engineered nanoparticles in suspensions and products, J. Anal. Atom. Spectrom. 26 (2011) 1701–1721, https://doi.org/10.1039/c1ja10071h.

[3] D.M. Mitrano, J.F. Ranville, A. Bednar, K. Kazor, A.S. Hering, C.P. Higgins, Tracking dissolution of silver nanoparticles at environmentally relevant concentrations in laboratory, natural, and processed waters using single particle ICP-MS (spICP-MS), Environ. Sci. Nano. 1 (2014) 248–259, https://doi.org/10.1039/C3EN00108C.

[4] F. Laborda, E. Bolea, J. Jiménez-Lamana, Single particle inductively coupled plasma mass spectrometry for the analysis of inorganic engineered nanoparticles in environmental samples, Trends Environ. Anal. Chem. 9 (2016) 15–23, https://doi.org/10.1016/j.teac.2016.02.001.

[5] D. Mozhayeva, C. Engelhard, A critical review of single particle inductively coupled plasma mass spectrometry – a step towards an ideal method for nanomaterial characterization, J. Anal. Atom. Spectrom. 35 (2020), https://doi.org/10.1039/C9JA00206E, 1740-1783.

[6] M.D. Montaño, J.W. Olesik, A.G. Barber, K. Challis, J.F. Ranville, Single Particle ICP-MS: advances toward routine analysis of nanomaterials, Anal. Bioanal. Chem. 408 (2016) 5053–5074, https://doi.org/10.1007/s00216-016-9676-8.

[7] J. Liu, K.E. Murphy, M.R. Winchester, V.A. Hackley, Overcoming challenges in single particle inductively coupled plasma mass spectrometry measurement of silver nanoparticles, Anal. Bioanal. Chem. 409 (2017) 6027–6039, https://doi.org/10.1007/s00216-017-0530-4.

[8] L. Hendriks, B. Ramkorun-Schmidt, A. Gundlach-Graham, J. Koch, R.N. Grass, N. Jakubowski, D. Günther, Single-particle ICP-MS with online microdroplet calibration: toward matrix independent nanoparticle sizing, J. Anal. Atom. Spectrom. 34 (2019) 716–728, https://doi.org/10.1039/C8JA00397A.

[9] E. Bolea-Fernández, D. Leite, A. Rua-Ibarz, L. Balcaen, M. Aramendia, M. Resano, F. Vanhaecke, Characterization of SiO2 nanoparticles by single particle-inductively coupled plasma-tandem mass spectrometry (SP-ICP-MS/MS), J. Anal. Atom. Spectrom. 32 (2017) 2140–2152, https://doi.org/10.1039/C7JA00138J.

[10] E. Bolea-Fernandez, D. Leite, A. Rua-Ibarz, T. Liu, G. Woods, M. Aramendia, M. Resano, F. Vanhaecke, On the effect of using collision/reaction cell (CRC) technology in single-particle ICP-mass spectrometry (SP-ICP-MS), Anal. Chim. Acta 1077 (2019) 95–106, https://doi.org/10.1016/j.aca.2019.05.077.

[11] A. Rua-Ibarz, E. Bolea-Fernandez, G. Pozo, X. Dominguez-Benetton, F. Vanhaecke, K. Tirez, Characterization of iron oxide nanoparticles by means of single-particle ICP-mass spectrometry (SP-ICP-MS) – chemical versus physical resolution to overcome spectral overlap, J. Anal. Atom. Spectrom. 35 (2020) 2023–2032, https://doi.org/10.1039/D0JA00183J.

[12] H.E. Pace, N.J. Rogers, C. Jarolimek, V.A. Coleman, C.P. Higgins, J.F. Ranville, Determining transport efficiency for the purpose of counting and sizing

nanoparticles via single particle inductively coupled plasma mass spectrometry, Anal. Chem. 83 (2011) 9361–9369, https://doi.org/10.1021/ac201952t.
[13] J.W. Olesik, P.J. Gray, Considerations for measurement of individual nanoparticles or microparticles by ICP-MS: determination of the number of particles and the analyte mass in each particle, J. Anal. Atom. Spectrom. 27 (2012) 1143–1155, https://doi.org/10.1039/C2JA30073G.
[14] M. Loula, A. Kaňa, O. Mestek, Non-spectral interferences in single-particle ICP-MS analysis_ an underestimated phenomenon, Talanta 202 (2019) 565–571, https://doi.org/10.1016/j.talanta.2019.04.073.
[15] S. Miyashita, H. Mitsuhashi, S. Fujii, A. Takatsu, K. Inagaki, T. Fujimoto, High transport efficiency of nanoparticles through a total-consumption sample introduction system and its beneficial application for particle size evaluation in single-particle ICP-MS, Anal. Bioanal. Chem. 409 (2017) 1–15, https://doi.org/10.1007/s00216-016-0089-5.
[16] B. Ramkorun-Schmidt, S.A. Pergantis, D. Esteban-Fernández, N. Jakubowski, D. Günther, Investigation of a combined microdroplet generator and pneumatic nebulization system for quantitative determination of metal-containing nanoparticles using ICPMS, Anal. Chem. 87 (2015) 8687–8694, https://doi.org/10.1021/acs.analchem.5b01604.
[17] D. Rosenkranz, F.L. Kriegel, E. Mavrakis, S.A. Pergantis, P. Reichardt, J. Tentschert, N. Jakubowski, P. Laux, U. Panne, A. Luch, Improved validation for single particle ICP-MS analysis using a pneumatic nebulizer/microdroplet generator sample introduction system for multi-mode nanoparticle determination, Anal. Chim. Acta 1099 (2020) 16–25, https://doi.org/10.1016/j.aca.2019.11.043.
[18] B. Meermann, V. Nischwitz, ICP-MS for the analysis at the nanoscale – a tutorial review, J. Anal. Atom. Spectrom. 33 (2018) 1432–1468, https://doi.org/10.1039/C8JA00037A.
[19] C. Agatemor, D. Beauchemin, Matrix effects in inductively coupled plasma mass spectrometry: a review, Anal. Chim. Acta 706 (2011) 66–83, https://doi.org/10.1016/j.aca.2011.08.027.
[20] C.A. Sötebier, D.J. Kutscher, L. Rottmann, N. Jakubowski, U. Panne, J. Bettmer, Combination of single particle ICP-QMS and isotope dilution analysis for the determination of size, particle number and number size distribution of silver nanoparticles, J. Anal. Atom. Spectrom. 31 (2016) 2045–2052, https://doi.org/10.1039/C6JA00137H.
[21] L. Telgmann, C.D. Metcalfe, H. Hintelmann, Rapid size characterization of silver nanoparticles by single particle ICP-MS and isotope dilution, J. Anal. Atom. Spectrom. 29 (2014) 1265–1272, https://doi.org/10.1039/C4JA00115J.
[22] J. Vidmar, T. Buerki-Thurnherr, K. Loeschner, Comparison of the suitability of alkaline or enzymatic sample pre-treatment for characterization of silver nanoparticles in human tissue by single particle ICP-MS, J. Anal. Atom. Spectrom. 33 (2018) 752–761, https://doi.org/10.1039/C7JA00402H.
[23] I. Abad-Alvaro, D. Leite, D. Bartczak, S. Cuello-Nunez, B. Gomez-Gomez, Y. Madrid, M. Aramendia, M. Resano, H. Goenaga-Infante, An insight into the determination of size and number concentration of silver nanoparticles in blood using single particle ICP-MS (spICP-MS): feasibility of application to samples relevant to *in vivo* toxicology studies, J. Anal. Atom. Spectrom. 36 (2021) 1180–1192, https://doi.org/10.1039/D1JA00068C.
[24] I. De la Calle, M. Menta, F. Séby, Current trends and challenges in sample preparation for metallic nanoparticles analysis in daily products and environmental samples: a review, Spectrochim. Acta Part B At. Spectrosc. 125 (2016) 66–96, https://doi.org/10.1016/j.sab.2016.09.007.
[25] E. Bolea, J. Jiménez-Lamana, F. Laborda, I. Abad-Álvaro, C. Bladé, L. Arola, J.R. Castillo, Detection and characterization of silver nanoparticles and dissolved species of silver in culture medium and cells by AsFlFFF-UV-Vis-ICPMS: application to nanotoxicity tests, Analyst 139 (2014) 914–922, https://doi.org/10.1039/C3AN01443F.
[26] W.-W. Lee, W.-T. Chan, Calibration of single-particle inductively coupled plasma-mass spectrometry (SP-ICP-MS), J. Anal. Atom. Spectrom. 30 (2015) 1245–1254, https://doi.org/10.1039/C4JA00408F.
[27] K.E. Murphy, J. Liu, A.R. Montoro Bustos, M.E. Johnson, M.R. Winchester, Characterization of Nanoparticle Suspensions Using Single Particle Inductively Coupled Plasma Mass Spectrometry, National Institute of Standards and Technology, 2016, https://doi.org/10.6028/NIST.SP.1200-21.
[28] S. Cuello-Nuñez, I. Abad-Álvaro, D. Bartczak, M.E. del Castillo Busto, D.A. Ramsay, F. Pellegrino, H. Goenaga-Infante, The accurate determination of number concentration of inorganic nanoparticles using spICP-MS with the dynamic mass flow approach, J. Anal. Atom. Spectrom. 35 (2020) 1832–1839, https://doi.org/10.1039/C9JA00415G.
[29] International Organization for Standardization-ISO, ISO/TS 19590:2017(E). Nanotechnologies — Size Distribution and Concentration of Inorganic Nanoparticles in Aqueous Media via Single Particle Inductively Coupled Plasma Mass Spectrometry, 2017.